Cation Binding and Conformation of Tryptic Fragments of *Nereis* Sarcoplasmic Calcium-Binding Protein: Calcium-Induced Homo- and Heterodimerization†

Isabelle Durussel,‡ Ying Luan-Rilliet,‡ Tatiana Petrova,‡ Takashi Takagi,§ and Jos A. Cox*,‡

Department of Biochemistry, University of Geneva, 1211 Geneva 4, Switzerland, and Biological Institute, Faculty of Science, Tohoku University, Sendai, Japan 980

Received October 1, 1992; Revised Manuscript Received December 16, 1992

ABSTRACT: *Nereis* sarcoplasmic calcium-binding protein (NSCP) is a compact 20-kDa protein that competitively binds three Ca^{2+} or Mg^{2+} ions and displays strong positive cooperativity. Its three-dimensional structure is known. It thus constitutes a good model for the study of intramolecular information transduction. Here we probed its domain structure and interaction between domains using fragments obtained by controlled proteolysis. The metal-free form, but not the Ca^{2+} or Mg^{2+} form, is sensitive to trypsin proteolysis and is preferentially cleaved at two peptide bonds in the middle of the protein. The N-terminal fragment 1–80 (T_{1-80}) and the C-terminal fragment 90–174 (T_{90-174}) were purified to electrophoretic homogeneity. T_{1-80}, which consists of a paired EF-hand domain, binds one Ca^{2+} with $K_a = 3.1 \times 10^5$ M^{-1}; entropy increase is the main driving force of complex formation. Circular dichroism indicates that T_{1-80} is rich in secondary structure, irrespective of the Ca^{2+} saturation. Ca^{2+} binding provokes a difference spectrum which is similar to that observed in the intact protein. These data suggest that this N-terminal domain constitutes the stable structural nucleus in NSCP to which the first Ca^{2+} binds. T_{90-174} binds two Ca^{2+} ions with $K_a = 3.2 \times 10^4$ M^{-1}; the enthalpy change contributes predominantly to the binding process. Metal-free T_{90-174} is mostly in random coil but converts to an α-helical-rich conformation upon Ca^{2+} binding. Ca^{2+} binding to T_{1-80} provokes a red-shift and intensity decrease of the Trp fluorescence but a blue-shift and intensity increase in T_{90-174}. Molecular sieving and covalent cross-linking experiments indicate that the isolated peptides T_{1-80}, T_{1-89}, and T_{90-174} form homodimers in the presence of Ca^{2+}. Near-UV difference spectrophotometry revealed that in T_{1-80} the major spectral change occurs from 0.5 to 1 Ca^{2+}/fragment, i.e., upon binding of the second Ca^{2+} in the homodimer. In T_{90-174} most of the UV spectral change occurs upon binding of the first Ca^{2+}. Electrophoresis of the mixture of T_{1-80} + T_{90-174} under nondenaturing conditions revealed that in the presence of Ca^{2+} a heterodimer is formed with a mobility close to that of the intact protein. Heterodimer formation is further confirmed by the fact that the emission fluorescence spectrum of the equimolar mixture T_{1-80} + T_{90-174} is different from that expected from the sum of the individual components. Although the electrophoretic mobility and Trp environment of the heterodimer is similar to that of intact NSCP, its ion affinities are impaired. In conclusion, the two domains of *Nereis* sarcoplasmic calcium-binding protein show, unlike those of calmodulin and troponin C, a strong tendency to self-association and heterodimerization. This may be the reason why this protein does not interact with foreign targets but functions only as an intracellular Ca^{2+}–Mg^{2+} buffer.

The affinity, selectivity, and cooperativity of cation binding to a protein is determined at two levels: (i) local folding forces stabilize the cation-binding domains; and (ii) interactive forces bring the different domains together in a well-defined geometry. For *Nereis* sarcoplasmic Ca^{2+}-binding protein, some insight about these interactions can be obtained from the available three-dimensional structure of the Ca^{2+}-bound state (Cook et al., 1991; Vijay-Kumar & Cook, 1992) combined with solution studies on the Ca^{2+}, Mg^{2+}, and metal-free state (Cox & Stein, 1981; Engelborghs et al., 1990; Luan-Rilliet et al., 1992). However, the protein is complex and rather big (20 kDa). One can simplify the studies through the use of fragments representing domains and subdomains of the protein. Using this "peptide approach", very useful information could be gathered on the single-site helix–loop–helix (also called EF-hand motif; Kretsinger, 1987) and the "two-site" domain or paired EF-hand structures (Kuznicki et al., 1981; Minowa & Yagi, 1984; Reid, 1990; Shaw et al., 1990; Kay et al., 1991).

Functional Ca^{2+}-binding domains of the EF-hand type are systematically organized in a pairwise fashion to form a two-sites domain of ca. 70 residues (Strynadka & James, 1989). Key elements in the structure are (i) a short β-pleated sheet extending between Ca^{2+}-binding loops of the two sites and (ii) hydrophobic contacts between opposing α-helices, which form the highly conserved hydrophobic core. Synthetic 34-residue peptides corresponding to site III (Shaw et al., 1990) or IV (Kay et al., 1991) or troponin C spontaneously dimerize upon binding of Ca^{2+} to form a two-site domain with a three-dimensional structure very similar to the C-terminal half of intact troponin C. This simple "two-site model", which nearly perfectly describes the folding of a half troponin C molecule, is not sufficient for the Ca^{2+}-buffering protein parvalbumin. Indeed, using fragments of parvalbumin, Permyakov et al. (1991) observed the formation of a noncovalent complex between domain AB and two-site domain CD*EF, accompanied by an increase of the affinity for Ca^{2+}. The authors suggest that a key element in this stabilization is the shielding

† This work was supported by the Swiss National Science Foundation Grant 31-28637.90.

* To whom correspondence should be addressed: Department of Biochemistry 30, Quai Ernest-Ansermet, 1211 Geneva 4, Switzerland. Télefax: 296102. Electronic mail: Cox@CGEUGE52.

‡ University of Geneva.

§ Tohoku University.

0006-2960/93/0432-2394$04.00/0

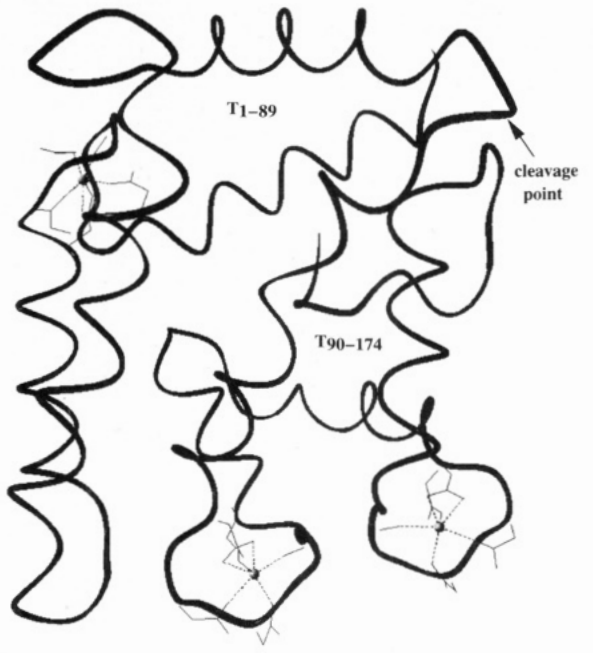

FIGURE 1: X-ray crystallographic structure of NSCP. The Ca^{2+} atoms in the functional binding sites I, III, and IV are represented by spheres, linked to the seven respective ligands. The cleavage point at Lys89 is indicated by an arrow.

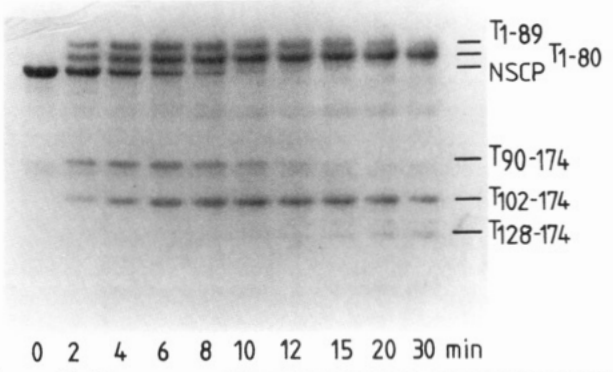

FIGURE 2: Time course of trypsin proteolysis of metal-free NSCP monitored by alkaline urea 12.5% polyacrylamide electrophoresis in the presence of 1 mM EGTA and 8 M urea. A solution of 1 mg/mL NSCP was digested with 1 μg/mL trypsin for the indicated times at 25 °C. The identity of the peptide bands, revealed by amino acid sequencing as described under Results, is indicated at the right, according to the numbering of the sequence (Collins et al., 1988).

of the hydrophobic core of domain CD*EF by the hydrophobic side of AB.

The C-terminal half molecule of NSCP bears structural resemblance to the CD*EF domain of parvalbumin (Vijay-Kumar & Cook, 1992). The N-terminal half is a two-site domain with a site I, which is structurally quite different from the one encountered in crystals of Ca^{2+}-binding proteins, and a site II that has lost its Ca^{2+}-binding capacity. The N- and C-terminal domains can clearly be distinguished, their polypeptide segments being not intertwined (Figure 1). However, they possess an extended contact zone, and the hydrophobic side chains of the N-terminal half neutralizing the hydrophobic core of the C-terminal half. NSCP[1] displays at least one degree of sophistication over parvalbumin, namely, the pronounced positive cooperativity in the binding of Mg^{2+}. This property classifies it in the select family of proteins with a T → R allosteric transition.

[1] Abbreviations: NSCP, *Nereis* sarcoplasmic calcium-binding protein; SDS, sodium dodecyl sulfate; DSS, disuccinimidyl suberate.

In the present study we probed the domain structure of NSCP by means of tryptic fragments corresponding to the N- and C-terminal two-site domains. We monitored the strong tendency of these fragments to reassociate into homodimers or heterodimers, leading in the latter case to a partially reconstituted NSCP. These studies are not immediately relevant to the presumed function of this abundant protein in muscle, namely, control of the Ca^{2+} fluxes and regulation of the free Mg^{2+} concentrations (Cox, 1990). However, they clearly provide insight in the principles of molecular design which orient proteins, composed of common structural building blocks, toward a function either as a Ca^{2+}–Mg^{2+} buffer or as a Ca^{2+}-regulated activator.

MATERIALS AND METHODS

Controlled Proteolysis of NSCP. Nereis SCP was purified as described by Engelborghs et al. (1990). The tryptic digestions of NSCP (1 mg/mL) were carried out at 25 °C in 20 mM NH_4HCO_3–NH_3, pH 8.5, containing 1 mM EGTA. Digestion was stopped by addition of 4 μg/mL soybean trypsin inhibitor followed by heating at 100 °C for 5 min. The tryptic fragments were separated on a DE52-cellulose column. Final purification was achieved by gel filtration and repeated ion exchange chromatography. The concentration of the fragments was determined by UV spectrophotometry using molar extinction coefficients of 21 100 for T_{1-80} and T_{1-89} and of 11 900 M^{-1} cm^{-1} for T_{90-174} and $T_{102-174}$. The latter values were measured on protein stock solutions whose concentrations were determined by amino acid analysis after acid hydrolysis (in quadruplicate).

Amino Acid Analysis and Sequence Determination. Peptide were hydrolyzed with gas of constant boiling HCl containing 0.2% phenol at 150 °C for 1 h. Amino acid analysis was performed on a Hitachi L8500 amino acid analyzer with the *o*-phthalaldehyde method. Amino acid sequences of protein and peptides were determined by using an automated sequencer (Applied BioSystem Model 477A on line with a Model 120A PTH analyzer).

Metal Ion Determination and Metal Removal. For removal of contaminating metals, the fragments were precipitated with 3% trichloroacetic acid in the presence of 1 mM EDTA and then passed through a 40 × 1 cm Sephadex G-25 column equilibrated in the assay buffer. The assay buffer was freed of contaminating metals by passage over an EDTA Sepharose column (Haner et al., 1984). Total Ca^{2+} and Mg^{2+} concentrations were determined with a Perkin-Elmer Cetus Instruments 2380 atomic absorption spectrophotometer.

Cation Binding. Ca^{2+} binding to the fragments was measured at 25 °C by the flow dialysis method of Colowick and Womack (1969) in 50 mM Tris-HCl, pH 7.5, and 150 mM KCl (buffer A). Protein concentrations were 10–30 μM. Constants were determined from the Scatchard plot.

Microcalorimetry. Microcalorimetric measurements were performed with an LKB 2277 microcalorimeter equipped with a flow device (Milos et al., 1986; Luan-Rilliet et al., 1992) at 25 °C in 50 mM Tris-HCl or PIPES-NaOH, pH 7.5, and 150 mM KCl. Solutions of 10–100 μM fragments and of appropriate concentrations of Ca^{2+} and Mg^{2+} were mixed at a flow-mix rate of 2 × 0.15 mL/min. The proton release at pH 7.5 was measured by microcalorimetry (Luan-Rilliet et al., 1992) using Tris and PIPES buffers. The standard enthalpy changes of protonation of Tris and PIPES are –47.5 and –11.5 kJ mol^{-1}, respectively (Beres & Sturtevant, 1971). In this study the experimental precision on the enthalpy values is 3%.

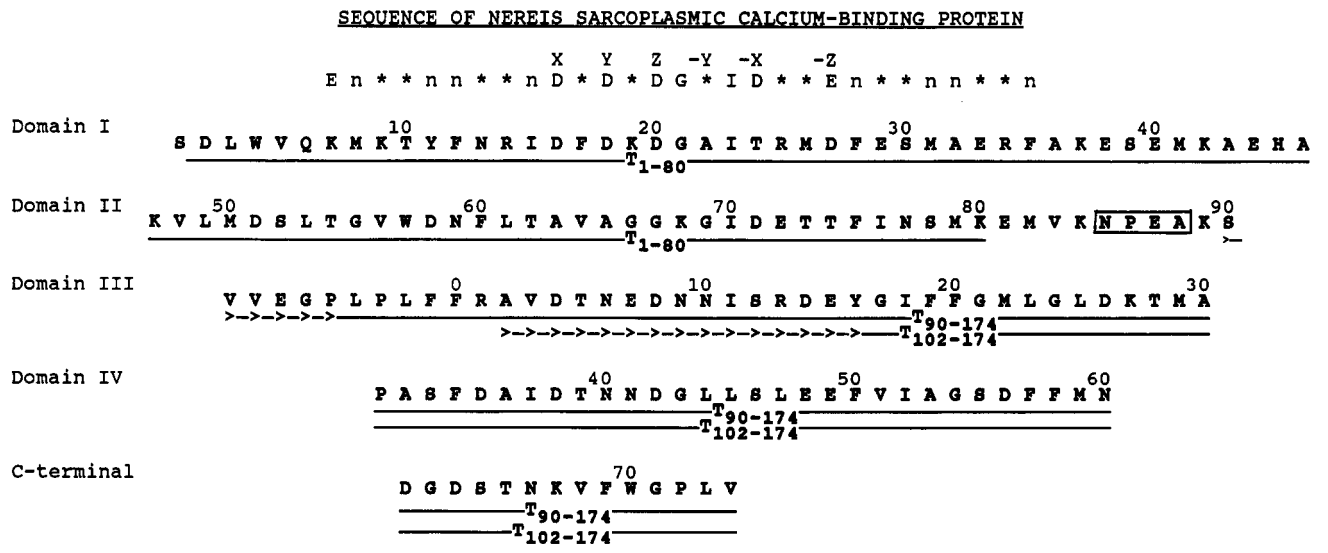

FIGURE 3: Trypsin cleavage points in NSCP. The sequence alignment according to the consensus sequence for EF hand domains (top) was taken from Cook et al. (1991). (>->->-) Automated sequencing of T_{90-174} and $T_{102-174}$. The sequence Asn-Pro-Glu-Ala, which forms a type I tight turn and is responsible for the compact shape of NSCP, is boxed.

Fluorimetry and Near-Ultraviolet Spectrophotometry. Emission fluorescence and UV absorption difference spectra were recorded with a Perkin-Elmer LS-5B spectrofluorimeter and a Perkin-Elmer Cetus Instruments lambda 5 spectrophotometer, respectively, both interfaced to a computer. Fluorescence measurements were carried out on metal-free solutions of 2 μM tryptic fragments at room temperature with excitation and emission slits of 5.0 nm. 500 μM EGTA, 2 mM $MgCl_2$, and 1 mM $CaCl_2$ were added subsequently to obtain the metal-free, Mg^{2+}, and Ca^{2+} forms, respectively. Difference spectra were recorded on solutions with a optical density at 280 nm of 1.5–2.5, corrected for the blank and for dilutions, and normalized to an optical density of 1.0.

Far-UV Circular Dichroism. Spectra were recorded at room temperature on a Jasco-20A spectropolarimeter equipped with a data processor. The instrument was calibrated with camphorsulfonate-d_{10} (Eastman, Rochester, NY). The peptide fragments (50 μM) were equilibrated in 50 mM Tris-HCl, pH 7.5, 150 mM KCl, and 100 μM EGTA. A 0.2-mm cell was used for measurements between 200 and 250 nm. 2 mM $MgCl_2$ and 1 mM $CaCl_2$ were added subsequently. Since at the present time no precise data can be collected below 200 nm, no attempt was made to estimate the secondary structure of the fragments.

Covalent Cross-Linking. Cross-linking experiments were performed at room temperature as described earlier (Staros, 1982; Giedroc et al., 1983). To solutions containing 50 mM HEPES, pH 7.5, 0.1 M NaCl and either 1 mM $CaCl_2$ or 1 mM EDTA and 18–28 μM fragments, and various concentrations (from 13 to 250 μM) of disuccinimidyl suberate were added. The stock solution of the cross-linking agent was freshly prepared in dry dimethylformamide. After 3 h of incubation, the reaction was stopped by the addition of ethanolamine to a final concentration of 1 mM. The reaction mixture was then subjected to electrophoresis in 16% polyacrylamide gels in the presence of 0.1% SDS (Laemmli, 1970), followed by staining with Coomassie Brilliant Blue.

Alkaline Electrophoresis. Polyacrylamide gel electrophoreses on 12.5% gels in the presence of either 1 mM Ca^{2+} or 1 mM EDTA were carried out as described by Head and Perry (1977) in the presence or absence of 8 M urea. When urea was absent, 10% glycerol was added to improve the migration.

RESULTS

Trypsinolysis and Fragment Preparation. Preliminary experiments of controlled trypsinolysis indicated that it is very difficult to cleave NSCP in the presence of Ca^{2+} or Mg^{2+}, but suitable digestion products are obtained in 1 mM EGTA with a trypsin to NSCP ratio of 1:1000. The time course (Figure 2) indicates that four stable peptides are generated. Sequence analyses (see below) indicated that in the order of increasing mobility the four new bands correspond to fragments 1–89, 1–80, 90–174, and 102–174, respectively.

A judicious adjustment of the trypsin/NSCP ratio and of the time of proteolysis allowed us to prepare samples enriched in any of the fragments. DE52-cellulose chromatography (Supplementary Material) could then be used to efficiently separate the N-terminal (eluting at 4 mM) and C-terminal fragments (eluting at 9–10 mM). By Q-Sepharose chromatography in the presence of 8 M urea (not shown) of the mixture of the two N-terminal fragments, microgram amounts of the fragment 1–89, named T_{1-89}, could be obtained in pure form. However, since the mixture of the two N-terminal fragments could not be readily separated, it was usually submitted to a second step of controlled proteolysis, which converted T_{1-89} into T_{1-80}. The two C-terminal peptides were separated by repeated DE52-cellulose chromatography. Three electrophoretically pure peptide fragments, named T_{1-80}, T_{90-174}, and $T_{102-174}$, were obtained in milligram amounts. The successful purification procedure necessitated repeated heat and/or trichloroacetic acid treatments, in order to suppress the reactivation of traces of contaminating trypsin.

Fragment Identification. Edman degradation showed that the α-amino group of T_{1-80} and T_{1-89} was blocked. Carboxypeptidase P digestion of T_{1-80} for 25 min revealed 0.9 mol of Lys and 0.7 mol of Met per mol of fragment, indicating that its C-terminal ended at Lys80. This was confirmed by amino acid analysis. T_{1-80} thus includes the first EF-hand plus most of the abortive site II (Figures 1 and 3). Carboxypeptidase P digestion of T_{1-89} for 5 min yielded 0.5 mol of Lys and 0.3 mol Ala per mol of fragment. Automated Edman degradation of T_{90-174} and $T_{102-174}$ yielded the sequences Ser-Val-Val-Glu-Gly- and Ala-Val-Asp-Thr-Asn-Glu-, respectively. Carboxypeptidase P digestion for 25 min revealed a C-terminal Val for both peptides. Since each contains a Trp

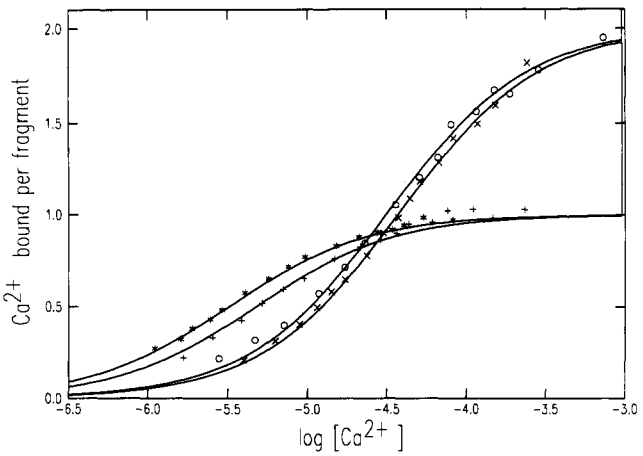

FIGURE 4: Ca^{2+} binding to T_{1-80} (*, +) and T_{90-174} (O, ×) in the absence (*, O) or presence (+, ×) of 2 mM Mg^{2+}. Ca^{2+} binding was measured by the flow dialysis method under conditions described earlier (Luan-Rilliet et al., 1992). Fragment concentrations were 25 μM. The solid lines are theoretical isotherms generated with the constants listed in Table I.

Table I: Ca^{2+}-Binding Parameters of Isolated T_{1-80}, T_{90-174}, and $T_{102-174}$

	$[Ca^{2+}]$/mol	K_a
no Mg^{2+}		
T_{1-80}	1	3.1×10^5 M^{-1}
T_{90-174}	2	3.2×10^4 M^{-1}
$T_{102-174}$	2	500 M^{-1}
+ 2 mM Mg^{2+}		
T_{1-80}	1	2.1×10^5 M^{-1}
T_{90-174}	2	2.7×10^4 M^{-1}

residue, it can be concluded that they encompass the C-terminus of NSCP. Hence, T_{90-174} comprises the entire domains III and IV (Figure 3), whereas $T_{102-174}$ contains part of domain III (the N-terminal α-helix is completely missing) and domain IV.

Ca^{2+} Binding to T_{1-80}, T_{90-174}, and $T_{107-174}$ Monitored by Flow Dialysis and Microcalorimetry. Figure 4 shows the Ca^{2+}-binding isotherms in the absence and presence of 2 mM Mg^{2+}. Table I summarizes the binding parameters of duplicate experiments. T_{1-80} binds one Ca^{2+} ion with $K_a = (3.1 \pm 0.8) \times 10^5$ M^{-1}, whereas T_{90-174} binds two Ca^{2+} ions noncooperatively with $K_a = (3.2 \pm 0.3)$ $10^4 \times M^{-1}$. 2 mM Mg^{2+} has a very small antagonistic effect on the Ca^{2+} affinities of both peptides. The binding of Ca^{2+} to $T_{102-174}$ is difficult to evaluate due to the low affinity: flow-dialysis yields a stoichiometry of two Ca^{2+} and a binding constant of ca. 5×10^2 M^{-1}, i.e., 1/500000-fold of that in native NSCP (data not shown).

Microcalorimetric experiments were carried out in duplicate at a saturating concentration of Ca^{2+} (500 μM) in two buffers of different protonation enthalpy (Table II). The proton release upon binding of Ca^{2+} to T_{1-80} amounts to 0.3 H^+/fragment; the standard enthalpy corrected for proton release equals −7.1 kJ/mol. Ca^{2+} binding to T_{1-80} is both enthalpy- and entropy-driven, with the entropy contribution being the major driving force. Ca^{2+} binding to T_{90-174} is accompanied by a release of 0.48 H^+/bound Ca^{2+}. The contribution of the enthalpy change is more significant, because T_{90-174} loses conformational entropy due to refolding upon Ca^{2+} binding (see later).

Homodimerization of Fragments T_{1-80}, T_{1-89}, and T_{90-174}. T_{1-80} and T_{90-174} eluted from a calibrated Sephadex G75 column (120 × 1 cm), equilibrated in 10 mM Tris-HCl, pH 7.5, and 1 mM $CaCl_2$, as discrete, narrow peaks with apparent molecular masses of 25 and 23 kDa, respectively. These unexpectedly high values (the monomer molecular masses deduced from the sequence are 9.2 and 9.7 kDa, respectively) suggest that the fragments form homodimers. To confirm the self-association of fragments, cross-linking experiments with DSS were performed. Fragments T_{1-80}, T_{1-89}, and T_{90-174} were incubated with the reagent at molar ratios from 5 to 10, and the reaction products were analyzed by electrophoresis in the presence of SDS. For each of the three fragments, one single covalent adduct of 18 kDa was formed in the presence of Ca^{2+}, thus pointing to highly specific homodimer formation (Figure 5). In the presence of 1 mM EDTA or 1 mM Mg^{2+}, no or very little cross-linked products were obtained. Pure $T_{102-174}$ does not form cross-linked products, even in the presence of Ca^{2+}.

Secondary Structure of T_{1-80} and T_{90-174}. The far-UV circular dichroic spectra of Ca^{2+}- and metal-free T_{1-80} and T_{90-174} are shown in Figure 6. A qualitative comparison with the reference spectra published by Johnson (1990) indicates that the metal-free form of T_{1-80} is already very structured with a predominance of α-helix; Ca^{2+} binding leads to very small changes. In contrast, the secondary structure of T_{90-174} is more sensitive to Ca^{2+} binding: starting with almost no discrete structure in the metal-free form, the fragment adopts an α-helix containing structure upon binding of Ca^{2+}. The α-helical content of the Ca^{2+}-loaded form is still much lower than in T_{1-80} or intact NSCP (Cox & Stein, 1981). In the presence of 2 mM Mg^{2+} (no Ca^{2+}), the two fragments display the same spectra as the metal-free forms (not shown).

Difference Spectrophotometry on T_{1-80} and T_{90-174}. Figure 7 shows the UV difference spectra of T_{1-80} and T_{90-174}. The "apo-denatured" and "Ca-apo" spectra of T_{1-80} are very similar to those of the intact protein, with the formation of a well-organized core containing the aromatic residues, when progressing from the denatured to the metal-free form, and exposure of Trp to a positively charged cleft or pocket when adopting the Ca^{2+}-filled conformation (intense negative band at 293 nm). The "apo-denatured" spectrum of T_{90-174} shows bands of low amplitude, confirming the observations in circular dichroism experiments that the conformation of metal-free T_{90-174} is close to the denatured state. The Ca^{2+}-induced spectrum shows two interesting zones: very strong positive Trp peaks at 281 and 285 nm and marked negative Phe peaks in the 240–270-nm zone. The Ca^{2+}-induced folding of the peptide leads to burying of the Trp and Phe residues. Interestingly, the difference spectra of the shorter $T_{102-174}$ are very similar to those of T_{90-174}, although it has a 500-fold lower affinity for Ca^{2+} (data not shown).

The spectra obtained by titration of the fragments with Ca^{2+} (Supplementary Material) show that perturbation of all three aromatic groups, Trp, Tyr, and Phe, is similarly affected. Figure 8 shows the Trp spectral change as a function of Ca^{2+} addition under stoichiometric Ca^{2+}-binding conditions. The titration profile of T_{1-80} is characterized by an inflection point at 0.5 Ca^{2+}/fragment instead of the expected leveling off at 1 Ca^{2+}/fragment. This behavior must be interpreted in the light of the dimerization of T_{1-80} (see Discussion). The case of T_{90-174} is very different: binding of the first Ca^{2+} provokes almost all the signal change. Similar Mg^{2+} titrations indicated that the three peptides bind Mg^{2+}, but with an estimated affinity constant of 100 M^{-1} (data not shown).

Fluorescence Properties of T_{1-80}, T_{90-174}, and $T_{102-174}$. Figure 9 shows the fluorescence spectra of T_{1-80} and T_{90-174} after excitation at 295 nm. The spectrum of metal-free T_{1-80} shows a maximum of 333 nm, and binding of Ca^{2+} decreased the signal with a concomitant red-shift of the maximum. These

Table II: Thermodynamic Parameters for Ca^{2+} Interaction with T_{1-80} and T_{90-174}

	ΔH_{Tris} (kJ mol^{-1})	ΔH_{Pipes} (kJ mol^{-1})	proton release[a]	ΔH_{Ca}[a,b] (kJ site^{-1})	ΔG_{Ca}[b,c] (kJ site^{-1})	Δs_{Ca}[b,c] (J K^{-1} site^{-1})	contribution of ΔH (%)
T_{1-80}	−21.5	−10.6	0.30	−7.1	−31.3	+81.2	23
T_{90-174}	−75.0	−40.0	0.97	−14.8	−25.7	+36.6	58

[a] Correction of the enthalpy values and evaluation of the amount of liberated protons is described in Luan-Rilliet et al. (1992). [b] Values are per metal binding site. [c] The standard Gibbs free energy change ($\Delta G°$) and entropy change ($\Delta S°$) were calculated with the equation: $\Delta G° = -RT \ln K_a = \Delta H° - T\Delta S°$, where R is the gas constant (= 8.31 J K^{-1} mol^{-1}) and T = 298.2 K.

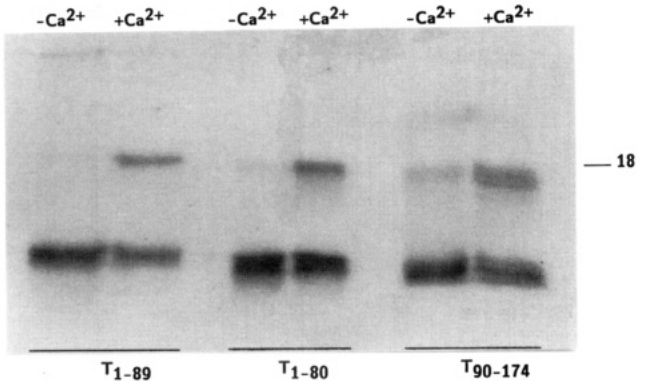

FIGURE 5: Demonstration of homodimer formation of T_{1-89}, T_{1-80}, and T_{90-174} by covalent cross-linking. The fragments were incubated with a DSS to protein fragment ratio of 5 (T_{1-89} and T_{1-80}) or 10 (T_{90-174}) for 3 h in the presence of 1 mM Ca^{2+} (+) or of 1 mM EDTA (−) and then submitted to electrophoresis in the presence of 0.1% SDS. At right the position of the 18-kDa molecular marker is indicated.

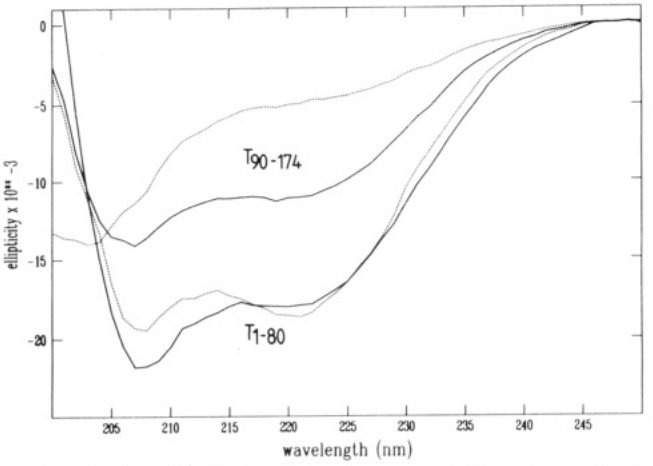

FIGURE 6: Far-UV circular dichroic spectra of T_{1-80} (lower lines) and T_{90-174} (upper lines) measured in a 0.2-mm cell at fragment concentrations of 50 μM, in the presence of 1 mM Ca^{2+} (—) or 0.1 mM EGTA (···).

data confirm that the metal-free form of T_{1-80} is already strongly structured with buried Trp4 and Trp57 and that Ca^{2+}-binding exposes the Trp residues to a polar environment, thus leading to quenching. The fluorescence properties of T_{1-89} are identical to those of T_{1-80} (not shown). By comparison, the spectrum of metal-free T_{90-174} shows a maximum at 352 nm, as does that of free Trp in water. Binding of Ca^{2+} increases the signal by 28% and leads to a blue-shift of the fluorescence maximum, suggesting that Ca^{2+}-induced folding leads to a partial burying of Trp170. Figure 9 also shows that in the presence of 2 mM Mg^{2+} (no Ca^{2+}) the two fragments display the same spectra as the metal-free forms. The shorter fragment $T_{102-174}$ behaves qualitatively as T_{90-174} (data not shown).

Ca^{2+}-Dependent Heterodimerization between T_{1-80} and T_{90-174}. The evidence of heterodimers formation was obtained using electrophoresis of the equimolar mixture of T_{1-80} and T_{90-174} under nondenaturating conditions. As shown in Figure

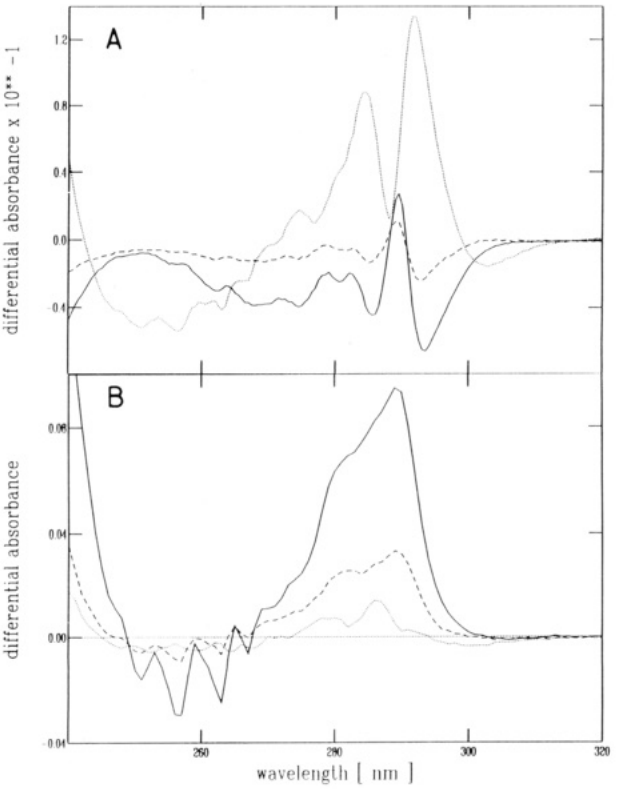

FIGURE 7: Ca^{2+}- and Mg^{2+}-induced difference spectra of T_{1-80} (A) and T_{90-174} (B) and a comparison of the metal-free and denatured form. Spectra were taken in 50 mM Tris-HCl, pH 7.5, and 150 mM KCl at room temperature. Ca^{2+}, Mg^{2+}, or guanidine hydrochloride were added up to 2.5 mM, 5 mM, and 3 M, respectively. (Solid line) Ca^{2+}-form, apo form; (dashed line) Mg^{2+}-form, apo form; (dotted line) apo form, denatured form.

10, in the presence of Ca^{2+} a new distinct protein band appears with a mobility close to that of the native protein. No such band is formed in the presence of EDTA, indicating that the formation of the heterodimer is Ca^{2+}-dependent. No complex has been observed for the $T_{1-80} + T_{102-174}$ mixture, underlining the importance of 90–102 fragment for maintaining the tertiary structure of NSCP's C-terminal part and/or ability to form stable dimers.

The equimolar mixture of metal-free T_{1-80} and T_{90-174} displays nearly the same fluorescence spectrum as that calculated from the sum of each of the two components (Figure 11). A similar result was obtained in the presence of 1 mM Mg^{2+} (data not shown). However, the experimental spectrum of the Ca^{2+}-loaded heterodimer shows a 35% higher intensity and a 7-nm blue-shift (thick solid line), as compared to the calculated spectrum (thin solid line). Thus, heterodimer formation of the Ca^{2+}-saturated fragments allows a more efficient burying of the Trp residues than in the homodimers. Circular dichroic spectra of the equimolar mixture of T_{1-80} and T_{90-174} are additive with those of the individual components (data not shown). Thus, heterodimer formation is *not* accompanied by a modification of the secondary structure of either of the two fragments.

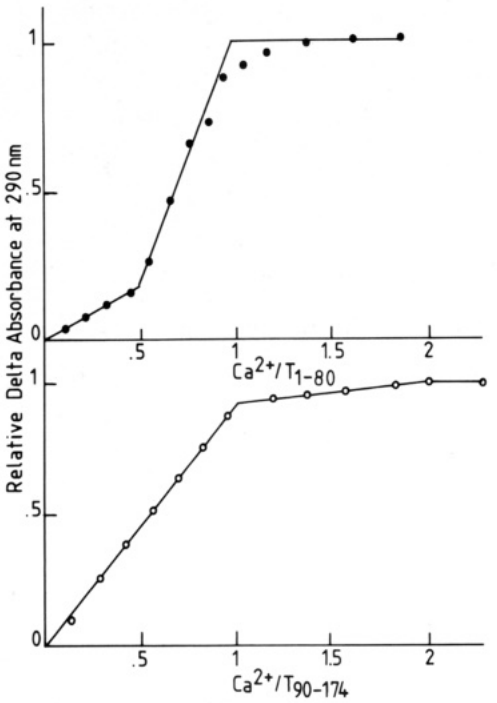

FIGURE 8: Ca^{2+} dependency of the spectral changes of T_{1-80} measured at 295 nm (●) and of T_{90-174} measured at 290 nm (○). The data were expressed as a fraction of the maximal spectral change.

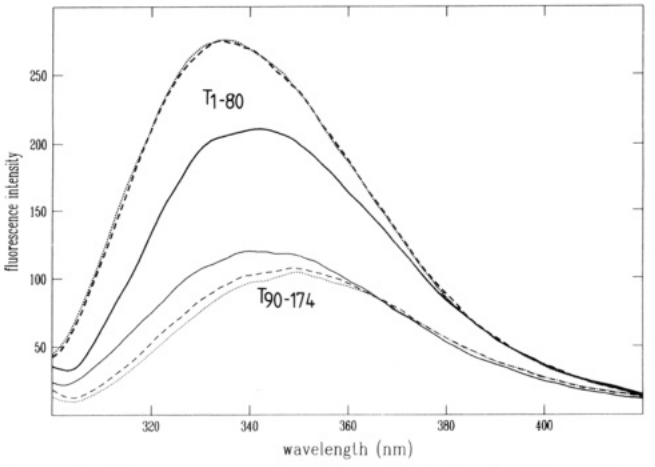

FIGURE 9: Fluorescence spectra of T_{1-80} (thick lines) or T_{90-174} (thin lines) in 50 mM Tris-HCl, pH 7.5, and 150 mM KCl at room temperature after excitation at 295 nm. The fragment concentration was 2 μM, in the presence of 2 mM Ca^{2+} (—), 2 mM Mg^{2+} (– – –), and 0.5 mM EGTA (···).

DISCUSSION

Metal-free NSCP is cleaved by controlled trypsinolysis into two fragments of almost the same size. The first cleavage point, Lys89, is located at the beginning of helix E (Figures 1 and 3), just beyond a type I tight turn which is responsible for the compact shape of NSCP in the Ca^{2+} form (Vijay-Kumar & Cook, 1992). Since the Ca^{2+} and Mg^{2+} forms of NSCP are very resistant to trypsinolysis, we assume that upon metal removal this segment becomes much more extended and prone to hydrolysis. In the presence of Ca^{2+}, the isolated fragments form homodimers, apparently because splitting of the strongly hydrophobic core of NSCP leaves the two halves with an unstable hydrophobic side; such domains seek stabilization by dimerization. Since the N- and C-terminal fragments of calmodulin and troponin C (Drabikowski et al., 1982; Tsalkova & Privalov, 1985) do not form homo- or heterodimers, it is interesting to examine the reason for this

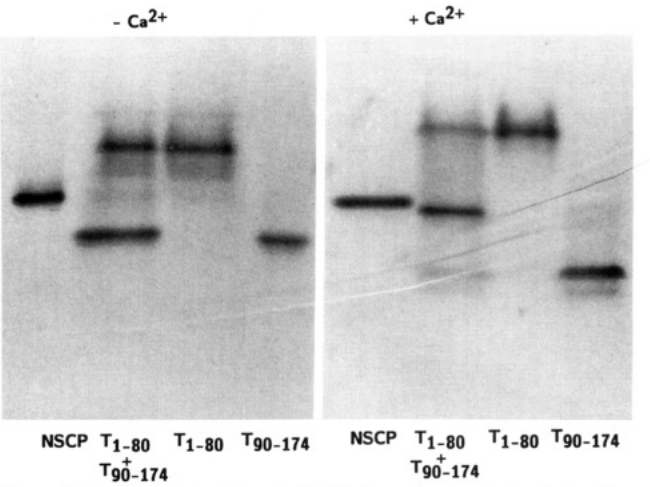

FIGURE 10: Demonstration of a Ca^{2+}-dependent complex formation between T_{1-80} and T_{90-174}. Intact NSCP (lane 1), the individual fragments T_{1-80} (lane 3), and T_{90-174} (lane 4) and the equimolar mixture of the fragments (lane 2) were preincubated in the presence of 1 mM EDTA ($-Ca^{2+}$) or 1 mM Ca^{2+} ($+Ca^{2+}$) and then submitted to alkaline electrophoresis in the presence of 10% glycerol.

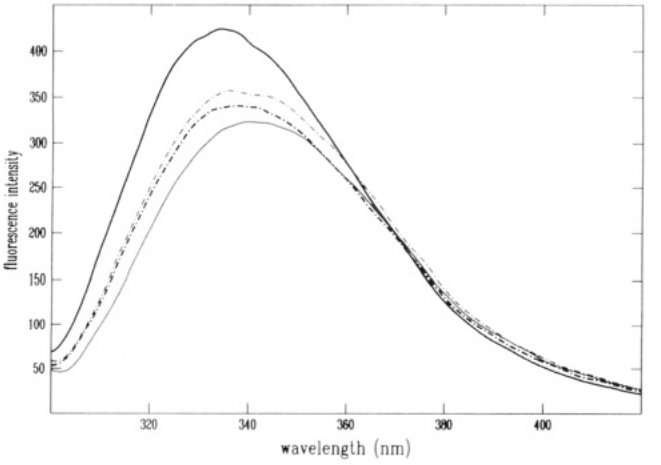

FIGURE 11: Fluorescence spectra of an equimolar mixture of 2 μM T_{1-80} + 2 μM T_{90-174} (thick lines) as compared to the sum of spectra (thin lines) of the individual compounds (see Figure 7). Conditions are as given in the legend to Figure 7, in the presence of 2 mM Ca^{2+} (—), 0.5 mM EGTA (–•–).

difference in behavior. The fragments of the latter proteins possess a negatively charged rim (Kretsinger et al., 1986), which leads to electrostatic repulsion between domains but favors attraction to positively charged amphiphilic peptides such as melittin (Comte et al., 1983) and the calmodulin-binding peptide segments found in target enzymes (Blumenthal et al., 1985). The domains of NSCP do not display such high density of charges on their rims, and the fragments do not interact with melittin (T. Petrova, unpublished observations).

T_{1-80}, the N-terminal fragment containing two EF-hand motifs, binds one Ca^{2+} exothermically with an affinity 500-fold lower than in intact NSCP. The secondary structure of this peptide is already very elaborate in the metal-free form; this may be due to the stabilizing effect of the empty second domain. Using difference spectrophotometry, one observes that the Trp environment undergoes a Ca^{2+}-induced change which is very similar to that observed in intact NSCP: Trp4 and/or Trp57 move toward a positively charged polar environment (Luan-Rilliet et al., 1992). This is confirmed by the fluorescence red-shift and intensity decrease. In Ca^{2+}-loaded NSCP the indole groups of Trp57 and Trp4 are oriented toward the surface, adjacent to the positive side chains of Lys7, Lys80, or Arg25. The conformational change as a

function of Ca^{2+} binding (Figure 8) suggests a model for the Ca^{2+}-linked dimerization: binding of Ca^{2+} to the monomeric T_{1-80} leads to a small change in the Trp environment, but binding Ca^{2+} to a second monomer allows the dimerization which provokes all the conformational change in both subunits of the homodimer.

T_{90-174} binds two Ca^{2+} exothermically with an affinity 5000-fold lower than in intact NSCP and 10-fold lower than in the N-terminal peptide. The latter is due to a reduced entropy contribution. Indeed, T_{90-174} possesses little secondary structure in the metal-free form, while it gains considerable α-helical structure upon Ca^{2+} binding. Consistent with this model, Trp170 moves into a hydrophobic environment with a fluorescence blue-shift and enhancement. Binding of the first Ca^{2+} provokes the full rearrangement in the Trp environment, and probably the dimerization process as well. This is somewhat reminiscent of the case of the synthetic peptide representing site III of troponin C: binding of Ca^{2+} leads to a conformational changes in the monomer followed by dimerization, conformational changes in the second subunit, and binding of a second Ca^{2+} without detectable conformational change (Shaw et al., 1990).

Whereas intact NSCP binds three atoms of Mg^{2+} with positive cooperativity and a mean intrinsic affinity constant of 2.6×10^4 M^{-1} (Luan-Rilliet et al., 1992), the isolated fragments do not noticeably interact with Mg^{2+}. If proteolysis leads to a similar decrease of the affinity for Mg^{2+} as for Ca^{2+}, the constant would be of the order of 10–50 M^{-1}. Difference spectrophotometry has indeed indicated that Mg^{2+} still weakly interacts with the fragments.

An important finding in this study is that upon mixing of the two fragments in the presence of Ca^{2+} the homodimers dissociate and subsequently reassociate to form one-to-one heterodimers in a very efficient way (Figure 10). The strict Ca^{2+} dependence is surprising, since metal-free NSCP already possesses an hydrophobic core (Luan-Rilliet et al., 1992), and one would expect that the metal-free fragments also tend to re-form this core. The partial reconstitution of the properties of intact NSCP is shown by the electrophoretic mobility and the Trp fluorescence properties of the heterodimer, which become similar to those in intact NSCP. The case is reminiscent of parvalbumin for which a Ca^{2+}-dependent complex of high affinity is formed between the CD–EF fragment and fragment AB (Permyakov et al., 1991). The Ca^{2+}-promoted transition from homodimers to a heterodimer must correspond to an increased stability. Indeed, the heterodimer likely has better complementary contact surfaces (as in intact NSCP) and more favorable electrostatic interactions. The fact that in NSCP and parvalbumin the two halves are so efficiently glued together determines the role of these proteins as intracellular Ca^{2+}–Mg^{2+} buffers.

ACKNOWLEDGMENT

We thank Dr. B. Schwendimann for the computer programs and Dr. Ph. Alard for helpful discussions.

SUPPLEMENTARY MATERIAL AVAILABLE

DE52 chromatographic profile of the trypsin digest of NSCP with electrophoresis of pure fragments; near-UV spectral Ca^{2+} titrations of T_{1-80} and T_{90-174} (5 pages). Ordering information is given on any current masthead page.

REFERENCES

Beres, L., & Sturtevant, J. M. (1971) *Biochemistry 10*, 2120–2125.
Blumenthal, D. K., Takio, K., Edelman, A. M., Charbonneau, H., Titani, K., Walsch, K. A., & Krebs, E. G. (1985) *Proc. Natl. Acad. Sci. U.S.A. 82*, 3187–3191.
Colowick, S. P., & Womack, F. C. (1969) *J. Biol. Chem. 244*, 774–777.
Collins, J., Cox, J. A., & Theibert, J. L. (1988) *J. Biol. Chem. 263*, 15378–15385.
Comte, M., Maulet, Y., & Cox, J. A. (1983) *Biochem. J. 209*, 269–272.
Cook, W. J., Ealick, S. E., Babu, Y. S., Cox, J. A., & Vijay-Kumar, S. (1991) *J. Biol. Chem. 266*, 652–656.
Cox, J. A. (1990) in *Stimulus–Response Coupling: The Role of Intracellular Calcium* (Dedman, J. R., & Smith, V. L., Eds.) pp 83–1070, CRC Press, Boca Raton, Ann Arbor, and Boston.
Cox, J. A., & Stein, E. A. (1981) *Biochemistry 20*, 5430.
Drabikowski, W., Brzeska, H., & Venyaninov, S. Y. (1982) *J. Biol. Chem. 257*, 11584–11590.
Engelborghs, Y., Mertens, K., Willaert, K., Luan-Rilliet, Y., & Cox, J. A. (1990) *J. Biol. Chem. 265*, 18809–18815.
Giedroc, D. P., Puett, D., Ling, N., & Staros, J. V. (1983) *J. Biol. Chem. 258*, 16–19.
Haner, M., Henzl, M. T., Raissouni, B., & Birnbaum, E. R. (1984) *Anal. Biochem. 138*, 229–234.
Head, F. G., & Perry, S. V. (1977) *Biochem. J. 137*, 145–154.
Johnson, W. C. (1990) *Proteins: Struct., Funct., Genet. 7*, 205–214.
Kay, L. E., Forman-Kay, J. D., McCubbin, W. D., & Kay, C. M. (1991) *Biochemistry 30*, 4323–4333.
Kretsinger, R. H. (1987) *Cold Spring Harbor Symp. Quant. Biol. 52*, 499–510.
Kretsinger, R. H., Rudnick, S. E., & Weissman, L. J. (1986) *J. Inorg. Biochem. 28*, 289–302.
Kuznicki, J., Grabarek, Z., Breska, H., Drabikowski, W., & Cohen, P. (1981) *FEBS Lett. 130*, 141–145.
Laemmli, U. K. (1970) *Nature 277*, 690–685.
Luan-Rilliet, Y., Milos, M., & Cox, J. A. (1992) *Eur. J. Biochem. 208*, 133–138.
Milos, M., Schaer, J.-J., Comte, M., & Cox, J. A. (1986) *Biochemistry 25*, 6279–6287.
Minowa, O., & Yagi, K. (1984) *J. Biochem. (Tokyo) 86*, 1175–1182.
Permyakov, E. A., Medvedkin, V. N., Mitin, Y. V., & Kretsinger, R. H. (1991) *Biochim. Biophys. Acta 1076*, 67–70.
Reid, R. E. (1990) *J. Biol. Chem. 265*, 5971–5976.
Shaw, G., Hodges, R. S., & Sykes, B. D. (1990) *Science 249*, 280–283.
Staros, J. V. (1982) *Biochemistry 21*, 3950–3955.
Strynadka, N. C. J., & James, M. N. G. (1989) *Annu. Rev. Biochem. 58*, 951–998.
Tsalkova, T. N., & Privalov, P. L. (1985) *J. Mol. Biol. 181*, 533–544.
Vijay-Kumar, S., & Cook, W. J. (1992) *J. Mol. Biol. 224*, 413–426.